Optical dielectric function of hydrogenated amorphous silicon: Tetrahedron model and experimental results

K. Mui and F. W. Smith
Department of Physics, The City College of the City University of New York, New York, New York 10031
(Received 7 March 1988)

A Si-centered tetrahedron model is developed for the determination of the effect of hydrogen on the visible–near-ultraviolet dielectric function ϵ of *a*-Si:H. Infrared-absorption and film-density measurements on the *a*-Si:H films studied here have been utilized to obtain the concentrations and relative fractions of the four tetrahedra, Si-$Si_{4-v}H_v$ ($v=0$–3), considered in the model and present in the films. These results have indicated that random bonding of hydrogen, with no excess of the dihydride Si-Si_2H_2 tetrahedron, occurs for *a*-Si:H films deposited at $T_s=250$ and 450 °C, but that nonrandom bonding with an excess of dihydride occurs for the $T_s=110$ °C film and for the annealed 250 °C film. The results of the Si-centered tetrahedron model have been used in the effective-medium approximation to obtain predictions for $\epsilon=\epsilon_1+i\epsilon_2$ that are in good agreement with experimental results presented here for the *a*-Si:H films studied. This model has thus been shown to provide a very useful framework for predicting ϵ_1 and ϵ_2 in the visible–near-uv region and for interpreting the nature of the bonding of hydrogen in these *a*-Si:H films.

I. INTRODUCTION

It is well known that the hydrogen bonded in hydrogenated amorphous silicon (*a*-Si:H) films has significant effects on the optical absorption of the films in both the infrared[1] (ir) and visible–near-ultraviolet[2,3] (uv) regions. These effects can be understood in terms of the presence of Si—H bonds in the films which give rise to characteristic absorption peaks in the ir due to stretching, bending, wagging or rocking, etc., modes. In the visible–near-uv region, the Si—H bonds can have both a direct alloying effect and an indirect network-relaxation effect on the optical absorption. It is important to understand these effects of hydrogen in detail so that correlations between both the observed ir and visible–near-uv optical absorption in *a*-Si:H films and the film microstructure, i.e., the local bonding configurations of Si and H atoms, can be established.

For this purpose a Si-centered tetrahedron model, previously applied by us to *a*-Si_xC_{1-x}:H (Ref. 4) and *a*-Si_xN_{1-x}:H (Ref. 5) alloys, is applied here to *a*-Si:H. Using this model, dielectric functions $\epsilon=\epsilon_1+i\epsilon_2$ are obtained for the four individual Si-centered tetrahedra expected to be present in the *a*-Si:H films (Si-$Si_{4-v}H_v$, $v=0$–3). Our measured ir-absorption and film-density results have been used to obtain information concerning the concentrations of these Si-centered tetrahedra for the *a*-Si:H films studied. These results are used along with the Bruggemann effective-medium approximation[6] (EMA) to make predictions for the dielectric functions of the *a*-Si:H films in the visible–near-uv region. The predictions of this Si-centered tetrahedron model are shown to be in good agreement with our experimental results for ϵ, thus indicating that the model provides a useful framework for understanding the direct alloying effect of hydrogen on the visible–near-uv optical absorption in *a*-Si:H films. We will also discuss the extent to which the bonding of hydrogen in these films is random.

In the next section results of previous ir and visible–near-uv optical absorption studies which provide information on the microstructure present in *a*-Si:H films are summarized. The Si-centered tetrahedron model is then developed, followed by details of the experimental procedures and analysis undertaken here. Results and discussion are then presented, including the comparison between the model predictions and experimental results.

II. BACKGROUND

Many experimental probes have been used in order to study the microstructure present in *a*-Si:H films. We will focus here on results obtained from ir absorption measurements and measurements of the dielectric function $\epsilon=\epsilon_1+i\epsilon_2$ in the visible–near-uv range.

Infrared absorption peaks due to the stretching, bending, and wagging modes of SiH_n ($n=1,2,3$) units have been widely studied, with a very useful review given recently by Cardona.[7] It is generally accepted that the stretching modes near 2000 cm^{-1} can provide information concerning the presence and concentrations of monohydride (Si-H), dihydride (Si-H_2), and trihydride (Si-H_3) units in the films. The peak observed nearest 2000 cm^{-1} is attributed to Si-H, the peak near 2090 cm^{-1} to Si-H_2 (and possibly Si-H in the presence of internal surfaces or voids),[8] and the peak near 2140 cm^{-1} to Si-H_3. The bending modes in the range from 840 to 900 cm^{-1} are attributed[9] to isolated Si-H_2 units or to $(Si\text{-}H_2)_n$ polymeric chains, with a possible contribution from Si-H_3 units if they are present in the films. The wagging modes near 640 cm^{-1} are believed[1] to arise from all three bonding units (Si-H_n, $n=1,2,3$).

Given the structural variability present in *a*-Si:H films prepared under different deposition conditions, it is practically impossible to develop a single structural model

which is applicable to all forms of *a*-Si:H. For example, it has in general not been possible to establish a quantitative correlation between the stretching modes near 2090 cm^{-1} and the bending modes present in films containing only Si-H and Si-H_2 units.[10] The 2090-cm^{-1} peak has been observed in films in which no bending modes were observed to be present, and it has been concluded that in such films this peak results from Si-H units at the inner surfaces of voids. Such behavior has been observed to be enhanced[10,11] in annealed *a*-Si:H films. In the absence of such internal surfaces, however, it may be assumed that only Si-H_2 units contribute to the 2090 cm^{-1} peak.

NMR studies, although not as detailed or sensitive as ir measurements, have given evidence[12] for a two-phase nature of the hydrogen bonding, namely dispersed (or isolated) hydrogen and clustered hydrogen. The clusters can contain from five to seven hydrogen atoms. Other workers have also proposed essentially two-phase models for the hydrogen incorporation: (1) Brodsky *et al.*[1] suggest that there exist two types of *a*-Si_xH_{1-x}, corresponding to dispersed hydrogen (*a*-Si:H) or to predominantly Si—H_2 and Si—H_3 bonding (*a*-SiH_x or silicon hydride); (2) Paul *et al.*[13] propose a structure consisting of grains (or islands) and grain boundaries (or tissues), with Si-H units present in the grains and $(Si\text{-}H_2)_n$ bonding dominating in the grain boundaries; and (3) Wagner *et al.*[8] propose a bulk amorphous network containing Si-H units and inner void surfaces where both Si-H and Si-H_2 units are present. It seems clear that these models share many similarities. We will take the point of view that hydrogen is randomly bonded in the bulk amorphous network, with nonrandom bonding corresponding to an enhanced probability for the existence of Si-H_2 units in the grain boundaries or at inner void surfaces.

Optical dielectric function measurements in the visible–near-uv range encompass both the absorption-edge region (about 1.5–2.5 eV) and the region where the main structure in ϵ, i.e., peaks in ϵ_1 and ϵ_2, occurs (about 2.5–4.5 eV). Extensive work by Aspnes and coworkers[14–16] on *a*-Si, and on as-deposited and annealed *a*-Si:H, has employed the EMA to model the measured ϵ_1 and ϵ_2 in terms of the possible components present in the amorphous films: *a*-Si, crystalline Si, and voids. This work has been very successful[14,15] in illustrating the role of density deficits in the films and the amorphous to crystalline transformation occurring under annealing. These studies have not, however, explicitly considered the effect of the bonded hydrogen on ϵ_1 and ϵ_2. Ewald *et al.*[3] have carried out a careful study of the energy dependence of ϵ_2 for *a*-Si:H films prepared at deposition temperatures from 27 to 400 °C. They present a qualitative discussion of their results for ϵ_2 in terms of the effect of hydrogen on the structure of the random network.

Many workers[2,17,18] have focused on changes observed in the absorption-edge region in *a*-Si:H films and have discussed the possible roles of hydrogen in causing these changes. These studies generally involve a correlation of the measured optical energy gap E_{opt}, with either the total hydrogen concentration or with the concentrations of Si-H and Si-H_2 units. It has not been possible to obtain a completely satisfactory correlation and it has been stated[18] that this is likely due to the dual roles of hydrogen in *a*-Si:H: (1) The direct alloying effect—hydrogen bonded in the film introduces Si—H bonds which are stronger than Si—Si bonds; and (2) the indirect network relaxation effect—the presence of hydrogen leads to the elimination or reconstruction of weak Si—Si bonds, thereby allowing the relaxation of the amorphous Si network. The former is a localized effect of hydrogen, while the latter is a nonlocalized effect. In the next section, a Si-centered tetrahedron model is developed in order to account for this direct alloying effect of hydrogen on ϵ_1 and ϵ_2. This model is not expected to give accurate predictions in the absorption-edge region where network relaxation is important. However, we anticipate that it may provide useful predictions for the overall structure of ϵ, including the magnitude and positions of peaks in ϵ_1 and ϵ_2.

III. TETRAHEDRON MODEL

The tetrahedron model to be presented for calculating ϵ_1 and ϵ_2 for these *a*-Si:H alloys considers Si-centered tetrahedra to be the fundamental structural units which determine the optical response of the films. This approach was first discussed by Philipp[19] for films based on silicon, oxygen, and nitrogen and was further developed by Aspnes and Theeten,[20] who combined it with the Bruggemann EMA for calculating the dielectric response of $Si_{1-x}(SiO_2)_x$ and $Si_{1-x}(SiN_{4/3})_x$ mixtures. It has since been successfully applied[4,5] to *a*-$Si_{1-x}C_x$ alloys. Although the use of the tetrahedron model for the visible–near-uv dielectric response of Si-based alloys has not been formally justified, successful comparisons[4,5,20] of its predictions with experimental results have established its usefulness. It is clear that tetrahedra are the largest structural units whose dielectric response can be treated within a simple framework. On the other hand, attempts to model the dielectric response on the basis of the next smallest structural unit, i.e., bonds (Si—H, Si—C, etc.), have been shown to be invalid in general.[4,5,20]

In this section the Si-centered tetrahedron model will be presented, and the probabilities P_v and dielectric functions ϵ_v of the individual Si-$Si_{4-v}H_v$ tetrahedra will be determined. This model will provide the framework, along with the Bruggemann EMA, for calculating the dielectric function ϵ in the visible–near-uv region for *a*-Si:H. Some predictions of this model will then be presented.

A. Model development

In the model as developed here, we will start by imposing some restrictions on the local atomic-bonding configurations to be considered in the alloys composed of Si and H atoms. Specifically, H—H bonds and Si-H_4 tetrahedra will not be considered since these species (i.e., H_2 and SiH_4 molecules) will not be part of the tetrahedral network. Thus, only the following four Si-centered tetrahedra will be included: Si-Si_4, Si-Si_3H, Si-Si_2H_2, and Si-SiH_3. Note that the last three tetrahedra correspond to the monohydride, dihydride, and trihydride Si—H_n ($n=1$–3) bonding configurations. Revesz[21] has pointed

out that these tetrahedra are the natural units to use in discussing *a*-Si:H films.

The probabilities P_v for the individual Si-Si$_{4-v}$H$_v$ (v=0–3) tetrahedra present in the films will depend both on the composition parameter x in these *a*-Si$_x$H$_{1-x}$ alloys and on the nature of the incorporation of hydrogen. We will start by assuming that the hydrogen is bonded completely randomly within the Si-centered tetrahedra, given that the Si-H$_4$ tetrahedron has already been excluded from consideration. Nonrandom bonding of hydrogen could correspond, for example, to an enhanced probability for the dihydride tetrahedron (Si-Si$_2$H$_2$) above that expected for the completely random bonding of hydrogen.

Since every Si atom must be bonded to at least one other Si atom in order to be part of the network, we will begin our consideration of bonding by focusing on the Si-Si$\equiv$ unit, where the second Si indicated is at the center of the tetrahedron. Following our previous presentation[4] for *a*-Si$_x$C$_{1-x}$ alloys, let f(Si)=x and f(H)=1−x be the corresponding atomic fractions within the *a*-Si$_x$H$_{1-x}$ film. Now,

$$f_1(\mathrm{Si}) = f(\mathrm{Si}) - f(\mathrm{Si})/4 - f(\mathrm{H})/4 = x - x/4 - (1-x)/4 = x - \tfrac{1}{4} \quad (1)$$

is the fraction of Si atoms which can bond to a Si-Si$\equiv$ unit. Note that f_1(Si) is less than f(Si) for two reasons: (1) f(Si)/4 is subtracted because this fraction of the Si atoms are *already* bonded in the Si-Si$\equiv$ units, and (2) f(H)/4 is subtracted because this fraction of the Si atoms will be bonded to H atoms, and thus will be effectively unavailable to bond to other Si atoms. It is clear that f_1(H)=f(H) is the fraction of H atoms which can bond to Si-Si$\equiv$ units since we have already excluded the possibility of H—H bonds in the films.

We now take into account the fact that each Si atom can have four bonds, whereas each H atom can have only one bond in the network in order to derive

$$f_2(\mathrm{Si}) = \frac{4f_1(\mathrm{Si})}{4f_1(\mathrm{Si}) + f_1(\mathrm{H})} = \frac{4x-1}{(4x-1)+(1-x)} = \frac{4x-1}{3x} , \quad (2)$$

as the fraction of *all* atoms which can bond to a Si-Si$\equiv$ unit which are Si atoms and

$$f_2(\mathrm{H}) = \frac{f_1(\mathrm{H})}{4f_1(\mathrm{Si}) + f_1(\mathrm{H})} = \frac{1-x}{3x} , \quad (3)$$

as the same fraction which are H atoms.

Now for the case of random bonding of hydrogen, let us consider as an example the probability P_2 (v=2) for a Si—Si$_2$H$_2$ or

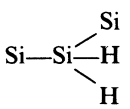

(dihydride) tetrahedron. We have that

$$P_2 = 3(1)^2 f_2(\mathrm{Si}) f_2^2(\mathrm{H}) = 3[(4x-1)/3x][(1-x)/3x]^2 . \quad (4)$$

The P_v for the four Si-centered tetrahedra are listed in Table I and shown in Fig. 1 as functions of x. Note that these P_v are not valid for x less than 0.25, at which point Si-H$_4$ tetrahedra or H—H bonds *must* be present in the films. In fact, solid *a*-Si$_x$H$_{1-x}$ films are not expected for $x < \frac{1}{3}$, the composition corresponding to polysilane, $(SiH_2)_n$. It is clear from Fig. 1 and the predictions of this model that dihydride units are expected to be present in these *a*-Si:H films even in the case of random bonding of hydrogen. The dihydride probability P_2 reaches 1% for x=0.85 and 5% for x=0.7 in this case.

The volume V_v associated with each Si-centered tetrahedron is also listed in Table I. These volumes have been calculated following the same procedure[4] outlined for the *a*-Si$_x$C$_{1-x}$ alloys, with the exception that we have added the Bohr radius a_B=0.529 Å to d(Si-H)=1.48 Å, the Si—H bond length, in order to account for the fact that the H atom (and its volume) is associated completely with the tetrahedon in which it is bonded.

The dielectric responses ϵ_v of the four Si-centered tetrahedra are, in general, not directly available from experiment. To derive them, we use the scaling approach of Aspnes and Theeten[20] along with the dielectric model of Phillips,[22] Van Vechten,[23] and Levine[24] (PVVL). The scaling approach is based on the expression

$$\epsilon_v(E) - 1 = C_{1v}[\epsilon_{a\text{-Si}}(C_{2v}E) - 1] , \quad (5)$$

where $\epsilon_v = \epsilon_{1v} + i\epsilon_{2v}$ is the dielectric function of the vth tetrahedron, E is the photon energy, C_{1v} and C_{2v} are the scaling parameters for the vth tetrahedron, and $\epsilon_{a\text{-Si}}$ is the dielectric function of amorphous Si in the absence of hydrogen (x=1). For $\epsilon_{a\text{-Si}}$ we use the data of Aspnes *et al.*[16] for chemical-vapor-deposited (CVD) *a*-Si, and we further take this to correspond to ϵ_v (v=0) for the Si-Si$_4$ tetrahedron.

We refer to our previous work[4] on *a*-Si$_x$C$_{1-x}$ for the details of the PVVL model, and only provide the results here. These are summarized in Table II, where $\langle r \rangle = (4-v)r(\mathrm{SiSi})/4 + vr(\mathrm{SiH})/4$, with r(SiSi)=1.176 Å and r(SiH)=0.74 Å. E_H and C are the homopolar (covalent) and heteropolar (ionic) parts of E_g, the average energy-gap parameter. The energy scaling parameter for the vth tetrahedron is given by

$$C_{2v} = E_g(a\text{-Si})/E_{gv} , \quad (6)$$

TABLE I. Tetrahedron probabilities P_v and volumes V_v for *a*-Si:H(Si$_x$H$_{1-x}$).

v	Tetrahedron	P_v	V_v (Å^3)
0	Si-Si$_4$	$\left[\frac{4x-1}{3x}\right]^3$	20.02
1	Si-Si$_3$H	$3\left[\frac{4x-1}{3x}\right]^2\left[\frac{1-x}{3x}\right]$	17.84
2	Si-Si$_2$H$_2$	$3\left[\frac{4x-1}{3x}\right]\left[\frac{1-x}{3x}\right]^2$	15.86
3	Si-SiH$_3$	$\left[\frac{1-x}{3x}\right]^3$	14.08

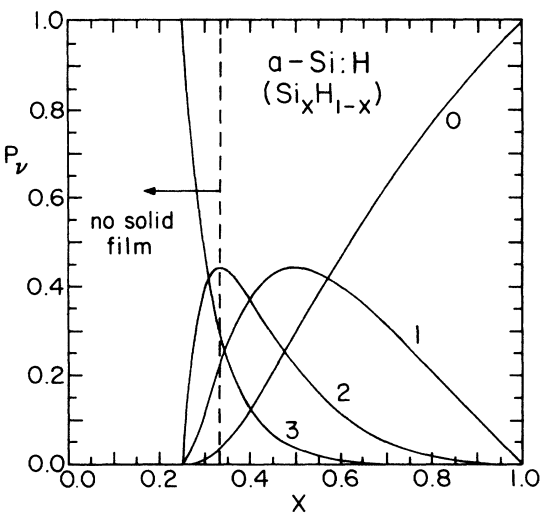

FIG. 1. Probabilities P_ν for Si-centered tetrahedra in a-Si:H (Si_xH_{1-x}) alloys as functions of composition x for the case of random bonding of hydrogen (see text). See Table I or II for numbering of the tetrahedra. Note that no solid a-Si:H film can exist for $x < \frac{1}{3}$.

while $C_{1\nu}$ is given by

$$C_{1\nu}=[n(\nu)/n(a\text{-Si})]C_{2\nu}^2 , \tag{7}$$

where $n(\nu)$ and $n(a\text{-Si})$ are the density of bonding electrons for the νth tetrahedron and for a-Si, respectively. We note that C for these Si-$Si_{4-\nu}H_\nu$ tetrahedra is always much less than E_H, so that effectively $E_g=E_H$. For the values of $E_g(a\text{-Si})$ and $n(a\text{-Si})$ to be used in Eqs. (6) and (7), we use values appropriate for the Si-Si_4 tetrahedron.

B. Model predictions

Making use of the values of $C_{1\nu}$ and $C_{2\nu}$ listed in Table II and the measured dielectric function data[16] for a-Si, $\epsilon_{a\text{-Si}}$, we have used Eq. (5) to generate scaled ϵ_ν spectra for the Si-centered tetrahedra. These are shown in Fig. 2, where it can be seen that the maxima in $\epsilon_{1\nu}$ and $\epsilon_{2\nu}$ decrease in magnitude and shift to higher energies as Si—Si bonds are replaced by stronger Si—H bonds. We note that the spectra displayed in Fig. 2 for the Si-Si_2H_2 tetrahedron are appropriate for polysilane, $(SiH_2)_n$.

Optical energy gaps E_{opt} for the tetrahedra, obtained from the spectra shown in Fig. 2 using both the constant-dipole-matrix-element plot ($\epsilon_2^{1/2}$ versus E) and the constant-momentum-matrix-element Tauc plot ($E\epsilon_2^{1/2}$ versus E), are presented in Table II, along with the energy range (in eV) over which the fits were obtained. The $\epsilon_2^{1/2}$ versus E plots consistently yielded much better fits than did the Tauc plots. A theoretical density-of-states calculation[25] has predicted a maximum attainable energy gap of about 3.0 eV for polysilane. This may be compared with the values of E_{opt} of 2.41 eV ($\epsilon_2^{1/2}$ versus E plot) and 3.09 eV (Tauc plot) for the Si-Si_2H_2 tetrahedron given in Table II.

As examples of the effects of hydrogen on the visible–near-uv dielectric function of a-Si:H as predicted by our model, we present in Fig. 3 ϵ_1 and ϵ_2 spectra for an a-$Si_{0.8}H_{0.2}$ alloy for two cases: (1) random bonding of hydrogen in the tetrahedra, and (2) all hydrogen bonding as dihydride, i.e., in Si-Si_2H_2 tetrahedra. These spectra have been determined using the Bruggemann EMA, defined by

$$\sum_i v_i \frac{\epsilon_i-\epsilon}{\epsilon_i+2\epsilon}0 , \qquad \sum_i v_i=1 , \tag{8}$$

where v_i and ϵ_i are the volume fraction and dielectric function, respectively, of the ith component and ϵ is the dielectric function of the effective medium. The components for our model are the Si-centered tetrahedra so that in Eq. (8) we set $\epsilon_i=\epsilon_\nu$ and $v_i=v_\nu$. The ϵ_ν for the tetrahedra are given in Fig. 2 and the v_ν are given by

$$v_\nu(x)=P_\nu(x)V_\nu \Big/ \left[\sum_\nu P_\nu(x)V_\nu\right] . \tag{9}$$

Here $P_\nu(x)$ and V_ν are the tetrahedron probabilities and volumes given in Table I, respectively, for the case of random bonding of hydrogen. It is apparent from Fig. 3 that the random bonding of hydrogen as primarily monohydride is more effective than complete dihydride bonding in shifting the absorption edge and peak in ϵ_2 to higher energies.

IV. EXPERIMENT AND ANALYSIS

The a-Si:H alloy films studied here were prepared in the capacitively coupled 13.56-MHz rf glow-discharge deposition system described previously.[4] The substrates, polished clear fused quartz for visible–near-uv measurements, oxygen-free high-conductivity (OFHC) copper for

TABLE II. Parameters for Si-centered tetrahedra (defined in text).

Tetrahedron	ν	$\langle r\rangle$ (Å)	E_H (eV)	C (eV)	E_g (eV)	C_2	C_1	Fit to $B(E-E_{\text{opt}})^2$: E_{opt} (eV)	Fitting range (eV)	Fit to $B'(E-E_{\text{opt}})^2/E^2$: E_{opt} (eV)	Fitting range (eV)
Si-Si_4	0	1.176	4.76	0	4.76	1	1	1.45	2.0–3.0	1.88	2.5–3.2
Si-Si_3H	1	1.067	6.06	0.14	6.06	0.785	0.864	1.85	2.3–3.6	2.38	3.2–3.4
Si-Si_2H_2	2	0.958	7.93	0.20	7.93	0.600	0.681	2.41	3.2–5.0	3.09	4.0–6.0
Si-SiH_3	3	0.849	10.69	0.28	10.69	0.445	0.493	3.25	4.0–6.0	3.49	5.4–6.0

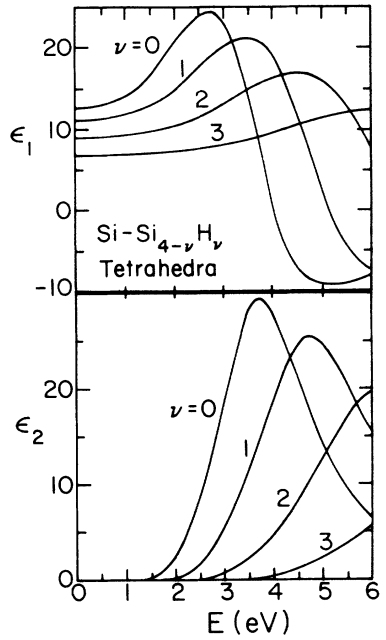

FIG. 2. Real part ϵ_1 and imaginary part ϵ_2 of the dielectric function vs energy E for Si-centered tetrahedra, obtained by scaling from amorphous Si (see text). See Table I or II for numbering of the tetrahedra.

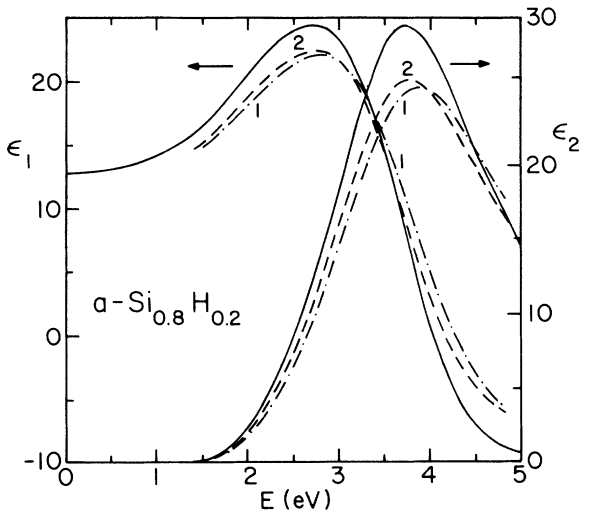

FIG. 3. Predicted values for the real part ϵ_1 and imaginary part ϵ_2 of the dielectric function vs energy E for a-$Si_{0.8}H_{0.2}$ obtained using the EMA (see text). Curve 1, random bonding of hydrogen; curve 2, all dihydride (Si-H_2). Solid curve is a-Si from Ref. 16.

density measurements, and intrinsic Si (resistivity of 2500 Ω cm) for infrared measurements, were mounted on the grounded, unpowered electrode. Undiluted silane (SiH_4, 99.95%, Linde) was used for the deposition, with typical parameters as follows: substrate temperature $T_s = 110$, 250, and 450 °C; discharge power of 7 W (0.15 W/cm^2); SiH_4 pressure of 0.075 Torr; and a SiH_4 flow rate of 72 sccm (cubic centimeters per minute at standard temperature and pressure). Deposition rates in the range 1.0–1.9 Å/sec were obtained. The low power and pressure employed here are important for obtaining high-quality a-Si:H films with a minimum of unwanted microstructure. The effect of varying T_s will be discussed below. Film thicknesses, from 300 to 13 000 Å, were determined optically.

The films studied are listed in Table III according to the substrate temperature T_s during deposition. Also indicated are subsequent annealing temperatures T_a and film-density results for the as-deposited films. Anneals were carried out for 1 h under flowing Ar in a tube furnace, while density measurements were undertaken on films removed from the Cu substrates using the flotation method in solutions of $ZnBr_2$ in H_2O. Infrared measurements were carried out using a Digilab FTS-40 FTIR

TABLE III. Properties of a-Si:H (Si_xH_{1-x}) films. Values in parentheses reflect results obtained using as-deposited film densities.

T_s (°C)	T_a (°C)	ρ[a] (g/cm^3)	E_{opt}[b] (eV)	N(Si-Si$_4$)[c] (10^{22} cm^{-3})	N(Si-H)[d] (10^{22} cm^{-3})	N(Si-H$_2$)[e] (10^{22} cm^{-3})	x	H (at. %)
110		2.14±0.03	1.72	3.58	0.848	0.125	0.805	19.5
250		2.20±0.03	1.71	3.86	0.770	0.055	0.842	15.8
250	350		1.45	(4.16)	0.464	0.072	(0.885)	(11.5)
250	400			(4.36)	0.295	0.046	(0.924)	(7.6)
250	400			(4.36)	0.295	0.046	(0.924)	(7.6)
250	450			(4.56)	0.127	0.020	(0.966)	(3.4)
250	500			(4.66)	0.052	0.004	(0.988)	(1.2)
250	550			(4.71)	0.0	0.0	1.0	0.0
450		2.29±0.03	1.57	4.44	0.452	0.0	0.915	8.5
450	550		1.43	(4.89)	0.0	0.0	1.0	0.0

[a]Film density.
[b]Obtained from a fit to $\epsilon_2(E) = B(E - E_{opt})^2$.
[c]Concentration of Si-Si$_4$ tetrahedra in film.
[d]Concentration of Si-H bonds (or Si-Si$_3$H tetrahedra) in film.
[e]Concentration of Si-H$_2$ bonds (or Si-Si$_2$H$_2$ tetrahedra) in film.

spectrophotometer in the range 400–4000 cm^{-1} in order to identify silicon-hydrogen bonding configurations and for the determination of the total bonded hydrogen content of the films.

Using our ir-absorbance results for the silicon-hydrogen stretching modes in the range 2000–2100 cm^{-1} along with the film density results, we have determined the probabilities (or number fractions) P_v for the Si-centered tetrahedra present in these films. For this purpose, the absorbance peak near 2000 cm^{-1} is attributed to the monohydride Si-Si_3H tetrahedron, while the absorbance peak near 2090 cm^{-1} is attributed to the dihydride Si-Si_2H_2 tetrahedron. There have been suggestions[8] that Si-H groups may also contribute to the 2090 cm^{-1} peak, and some evidence for this is found in the annealed samples. We will assume, however, that only Si-H_2 groups contribute at 2090 cm^{-1} in our as-deposited films. This assumption is in agreement with our observed ir absorption results in that we find the total area of the Si-H_2 bending mode peaks near 845 and 880 cm^{-1} to be directly proportional, to within experimental error, to the area of the 2090 cm^{-1} peak in the as-deposited films. Using a cross section[26] for these stretching modes of 1.4×10^{20} cm^{-2}, the concentrations N(Si-H) and N(Si-H_2) for these two tetrahedra have been determined from the measured absorbances A using the expression

$$N(\text{Si-H}_n)=1.4\times10^{20}\left[\frac{2.303}{d\langle\nu\rangle}\right]\int A(\nu,\text{Si-H}_n)d\nu\ , \quad (10)$$

where d is the film thickness, $\langle\nu\rangle$ is the peak wave number of the mode, and the integration is carried out over the absorbance peak. These integrations were carried out as part of the deconvolution procedure, illustrated in Fig. 4, where the absorbance data were fitted to a sum of two Gaussian peaks. No evidence was found from the ir data for any significant absorbance above the 2090-cm^{-1} peak which might be attributed to stretching modes of trihydride Si-SiH_3 tetrahedra. The total concentration of hydrogen atoms bonded in the films has been obtained from the integrated areas under both the stretching (2000–2100-cm^{-1}) peak and the wagging (635-cm^{-1}) absorption peaks. The results agree with each other to within 20%.

In order to determine the concentrations N(Si) of Si atoms in the film, the following expression for the film density ρ is used,

$$\rho=m_{\text{H}}N(\text{Si-H})+2m_{\text{H}}N(\text{Si-H}_2)+m_{\text{Si}}N(\text{Si})\ , \quad (11)$$

where m_{H} and m_{Si} are the atomic masses of H and Si, respectively. After obtaining N(Si) from Eq. (11) using our results for ρ, N(Si-H) and N(Si-H_2), the concentration of Si-Si_4 tetrahedra in the films can be found using the expression

$$N(\text{Si-Si}_4)=N(\text{Si})-N(\text{Si-H})-N(\text{Si-H}_2)\ . \quad (12)$$

For the determination of the dielectric functions $\epsilon=\epsilon_1+i\epsilon_2$ of these a-Si:H films, measurements of reflectances from the air and substrate sides of the film as well as film transmittance were undertaken using a Perkin Elmer Lambda 3 spectrophotometer in the range of photon energy from 1.45 to 4.86 eV. Details of the analysis procedure yielding n and k, the real and imaginary parts of the index of refraction, and film thickness d have been given in an earlier paper.[4] Values for the optical energy-gap parameter have been obtained for these films using a plot of $\epsilon_2^{1/2}$ versus E in the range from 2.0 to 2.7 eV.

V. RESULTS AND DISCUSSION

The infrared absorption and film-density results for these a-Si:H films will be presented first. The ir results have been used to obtain the concentration of monohydride (Si-H) and dihydride (Si-H_2) bonding configurations in the films, corresponding to the Si-Si_3H and Si-Si_2H_2 tetrahedra, respectively. Using the film-density results along with the derived Si-H and Si-H_2 concentrations, the concentrations of Si-Si_4 tetrahedra in the films have been obtained. In this way the relative probability fractions P and volume fractions v of the Si-centered tetrahedra will be determined. The results of the dielectric function measurements on these films in the 1.45–4.86-eV range will then be presented. A comparison between these experimental results for ϵ, and the predictions of the EMA employing the Si-centered tetrahedron model will then be given.

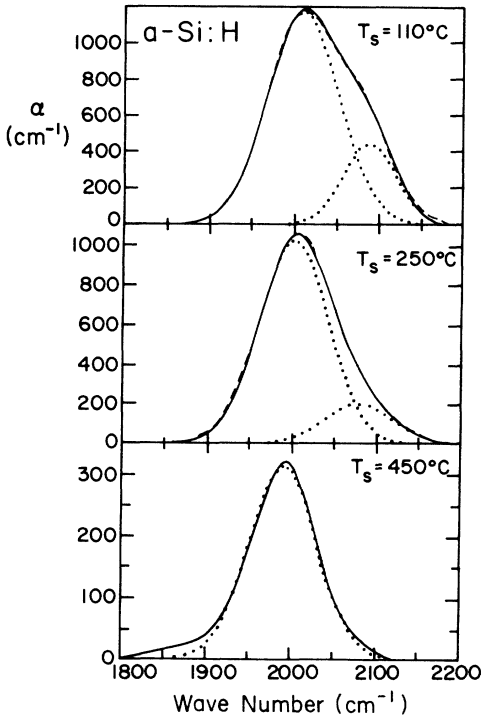

FIG. 4. Absorption coefficient α vs wave number for the Si-H_n stretching modes for the as-deposited T_s=110, 250, and 450 °C a-Si:H films. Also shown are the deconvolutions into separate Si-H and Si-H_2 peaks near 2005 and 2085 cm^{-1}, respectively. Solid curves are experimental results, while dotted and dashed curves are fitted peaks and their sums, respectively.

A. ir absorption and film density

Absorption peaks in the ir have been observed at or near the following wave numbers for the films listed in Table III, with specific peak positions showing small but systematic shifts[27] with deposition temperature T_s and annealing temperature T_a: (1) Si-H_n stretching modes at 2005 and 2085 cm^{-1}, with full widths at half maximum (FWHM's) of from 80 to 100 cm^{-1}; (2) Si-H_n bending modes at 845 and 880 cm^{-1}, with FWHM's of 30–55 cm^{-1}; and (3) Si-H_n wagging modes at 635 cm^{-1}, with FWHM's of from 60 to 120 cm^{-1}. No evidence for absorption near 2140 cm^{-1} corresponding to trihydride (Si-H_3) units or in the region from 1000 to 1100 cm^{-1} corresponding to Si—O bonds was observed.

In Fig. 4 the Si-H_n stretching mode peaks tor the as-deposited ($T_s=110$, 250, and 450 °C) films are presented, with the deconvolution into separate peaks near 2005 and 2085 cm^{-1} also shown. The fits with two peaks are very good for the $T_s=110$ and 250 °C films, while a single peak gives a reasonable fit for the $T_s=450$ °C film. In Table III are presented the measured film densities, the derived concentrations N(Si—H) of Si—H bonds, N(Si—H_2) of Si—H_2 bonds, and N(Si-Si_4) of Si-Si_4 tetrahedra, along with the corresponding film compositions x and hydrogen percentages. Results are also presented in Table III for N(Si-H) and N(Si-H_2) for the annealed films. Since film densities were not remeasured after annealing, the derived parameters in Tables III and IV which are enclosed in parentheses were determined using the as-deposited film densities and thus are not as accurate.

It is clear from Fig. 4 and Table III that N(Si-H), N(Si-H_2), and the hydrogen percentage in the films decrease with increasing T_s and T_a, while the film density and N(Si-Si_4) increase with increasing T_s. Following the $T_a=550$ °C anneals for both the $T_s=250$ and 450 °C films, no evidence for hydrogen remaining in the films could be obtained from these ir measurements.

In Table IV the derived results for the tetrahedron probabilities P_v and volume fractions v_v are given, along with the resulting void volume fraction $v_{void}=1-\sum_v v_v$. The P_v are obtained from the individual tetrahedron contributions N_v given in Table III, normalized to their total, i.e., $P_v=N_v/\sum_v N_v$. The v_v are obtained using $v_v=N_v V_v$, where the appropriate V_v are given in Table I. The variations of the probabilities P_v and the volume fractions v_v with T_s and T_a follow directly from the variations of the corresponding tetrahedron concentrations N_v. The increase of v_{void} and the reduction of film density with decreasing T_s can be associated with the increasing concentration of hydrogen bonded in the films. Hydrogen acts as a network terminator, thereby increasing the disorder in the films.

In order to determine the extent to which the hydrogen is randomly bonded in these films, we plot in Fig. 5 the tetrahedron probabilities P_v determined from the as-deposited and annealed films as functions of the composition parameter x in the experimentally available range from $x=0.75$ to 1.0. We find quite good agreement between the P_v determined for the as-deposited $T_s=250$ and 450 °C films and the P_v predicted by the Si-centered tetrahedron model for the case of completely random bonding of hydrogen, also shown in Fig. 5. For the $T_s=110$ °C and for the annealed $T_s=250$ °C films, however, it can be seen that there is a considerable enhancement of the Si—H_2 bonding probability, by factors of from 1.5 to 8, above that expected for the case of random bonding. We note that the lack of any evidence for Si-H_3 bonding configurations in these films is also consistent with the random bonding of hydrogen, as Si-H_3 is not expected to be at all significant except for $x<0.7$ (see Fig. 1).

This analysis of the microstructure present in these films using our results for the Si-H_n stretching modes and film density thus provides the following results: (1) for the $T_s=250$ and 450 °C as-deposited films, the hydrogen bonding is random and (2) for the $T_s=110$ °C and annealed $T_s=250$ °C films, the hydrogen bonding is nonrandom, with an enhancement of the probability for Si-H_2 bonding units.

Additional information concerning the hydrogen bonding in these films can be obtained from our results for the Si-H_2 bending modes at 845 and 880 cm^{-1}. With annealing, the total area $A(845)+A(880)$ of these peaks decreases while the ratio $A(845)/A(880)$ increases from 0.25 for $T_s=250$ °C to 0.67 for $T_a=400$ °C. This ratio is equal to 0.33 for the $T_s=110$ °C film. Also, the SiH_2 stretching

TABLE IV. Tetrahedron probabilities P_v and volume fractions v_v. Values in parentheses reflect results obtained using as-deposited film densities.

T_s (°C)	T_a (°C)	P_0 (Si-Si_4)	P_1 (Si-Si_3H)	P_2 (Si-Si_2H_2)	v_0 (Si-Si_4)	v_1 (Si-Si_3H)	v_2 (Si-Si_2H_2)	v_{void}
110		0.786	0.186	0.0275	0.716	0.151	0.020	0.113
250		0.824	0.164	0.0118	0.773	0.137	0.009	0.081
250	350	(0.886)	(0.099)	(0.0154)				
250	400	(0.928)	(0.063)	(0.0097)				
250	450	(0.969)	(0.027)	(0.0041)				
250	500	(0.988)	(0.011)	(0.0008)				
250	550	1.0	0.0	0.0				
450		0.907	0.092	0.0	0.889	0.080	0.0	0.030
450	550	1.0	0.0	0.0				

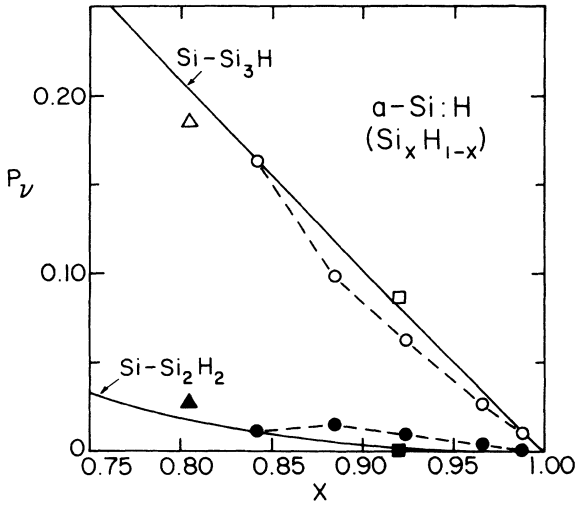

FIG. 5. Comparison between measured and predicted probabilities P_v for Si-centered tetrahedra in a-Si:H (Si_xH_{1-x}) alloys as functions of composition x. The solid curves are the predictions for random bonding of hydrogen from Fig. 1, while the triangles for the as-deposited $T_s=110$ °C, circles for the as-deposited (and annealed) $T_s=250$ °C, and squares for the as-deposited $T_s=450$ °C films represent experimental results.

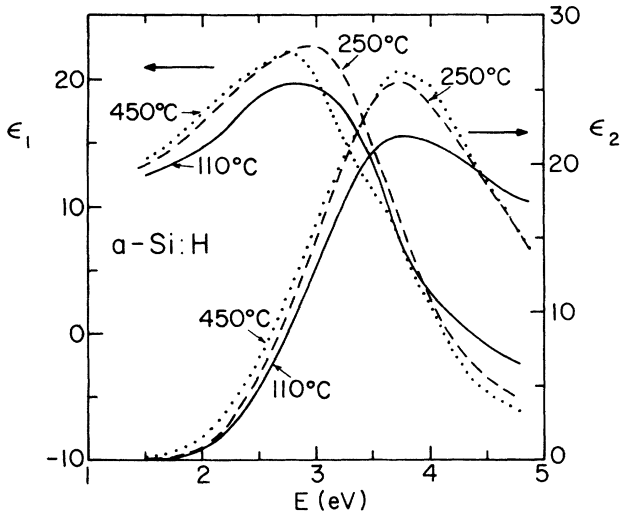

FIG. 6. Real part ϵ_1 and imaginary part ϵ_2 of the dielectric function vs energy E, measured for the as-deposited $T_s=110$, 250, and 450 °C a-Si:H films.

mode wave number increases from 2084 to 2088 cm^{-1} following the $T_a=350$ °C anneal. Both of these results are consistent[9] with the formation of $(SiH_2)_n$ chains, i.e., clustered SiH_2 units, with annealing. For the $T_a=350$ °C anneal, the film thickness was observed to increase, which is consistent with a decreasing film density related to the observed formation of $(SiH_2)_n$ units. These results thus show that the nonrandom hydrogen bonding observed in the $T_s=110$ °C and annealed $T_s=250$ °C films can be associated with the formation of either polymeric $(Si\text{-}H_2)_n$ or clustered SiH_2 units. We cannot, however, exclude the possibility that clustered Si-H units may contribute to the 2085-cm^{-1} stretching peak in the annealed films.

B. Visible–near-uv absorption

We first present our results for the dielectric function $\epsilon=\epsilon_1+i\epsilon_2$ from 1.45 to 4.86 eV for these as-deposited films, along with values for the optical energy gap E_{opt}. We then present the results of a comparison between the measured ϵ and the predictions of the EMA using the Si-centered tetrahedron model.

1. Results

In Fig. 6 ϵ_1 and ϵ_2 for the as-deposited $T_s=110$, 250, and 450 °C films are presented as functions of energy E. These results indicate greater disorder in the 110 °C film as the maxima in ϵ_1 and ϵ_2, while of lower magnitude, are broader than for the 250 and 450 °C films. Values of E_{opt} are presented in Table III, where it can be seen that E_{opt} decreases with increasing T_s or T_a, i.e., with decreasing hydrogen content, in agreement with the results of other workers.[2,17,18]

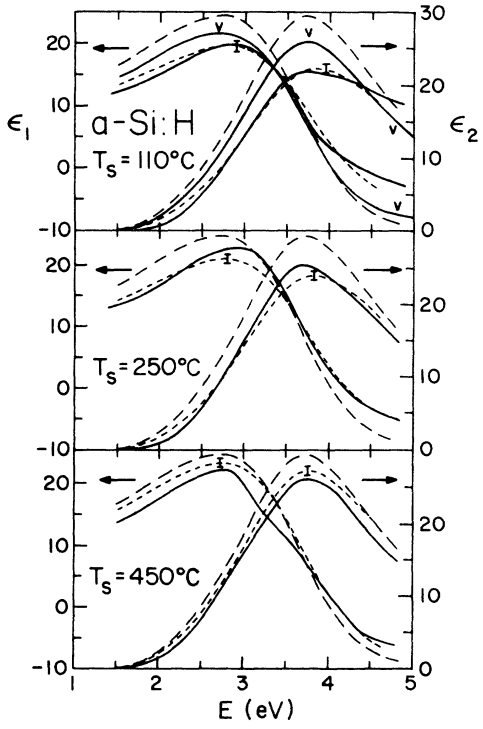

FIG. 7. Comparison between measured and predicted real part ϵ_1 and imaginary part ϵ_2 of the dielectric function for the as-deposited $T_s=110$, 250, and 450 °C a-Si:H films. Solid curve, experiment results for a-Si:H (this work); short-dashed curve, prediction of Si-centered tetrahedron model with EMA; long-dashed curve, results of Aspnes *et al.* for a-Si (Ref. 16). Uncertainties in the predicted ϵ_1 and ϵ_2 due to uncertainties in the measured film densities (see Table III) are indicated by the vertical bars near the peaks of ϵ_1 and ϵ_2. The curves labeled v for the $T_s=110°$ film represent the predictions of the EMA when it is assumed that the incorporated hydrogen simply leads to voids in the film (see text).

2. *Comparison with EMA prediction*

In order to test whether the Si-centered tetrahedron model developed here for *a*-Si:H can provide a useful framework for understanding and predicting the ϵ_1 and ϵ_2 spectra for these *a*-Si:H films, the EMA expressed by Eq. (8) will be used to generate results for ϵ_1 and ϵ_2 using as inputs the volume fractions v_v and v_{void} from Table IV and the dielectric function spectra for the individual Si-centered tetrahedra from Fig. 2. It should be emphasized that the volume fractions v for the Si-centered tetrahedra and v_{void} for the void component have been derived from ir absorption and density measurements on these films, while the ϵ_v are predictions of the Si-centered tetrahedron model.

The EMA predictions for ϵ_1 and ϵ_2 are presented in Fig. 7 along with the experimental results for the as-deposited 110, 250, and 450 °C films. Also shown are the data of Aspnes *et al.*[16] for hydrogen-free *a*-Si, for reference. The uncertainties shown for the EMA predictions reflect variations resulting from the uncertainty in the measured film densities (see Table III). The agreement between the predicted and measured values of ϵ_1 and ϵ_2 is quite good for the 110 °C film, and is satisfactory for the 250 and 450 °C films. We have also obtained predictions for ϵ_1 and ϵ_2 by assuming that the incorporated hydrogen simply leads to a density deficit, i.e., voids, in the film, as suggested by Aspnes *et al.*[20] This is illustrated in Fig. 7 for the 110 °C film. This approach, however, underestimates the effect of hydrogen on the observed decreases in ϵ_1 and ϵ_2 by at least a factor of 2, and thus does not correctly describe the role of hydrogen in these films.

It is clear from Fig. 7 that the $T_s = 110$ and 250 °C *a*-Si:H films studied here have absorption edges for ϵ_2 which are sharper than those predicted by the Si-centered tetrahedron model. Although the model is successful in predicting the overall shape of the ϵ_1 and ϵ_2 spectra, the inability of the scaling procedure to reproduce the absorption edges is an indication that the hydrogen bonded in the films is especially effective in reducing absorption in the gap and band tail regions. This is in accord with the current understanding of the role of hydrogen in *a*-Si:H.

VI. CONCLUSIONS

A Si-centered tetrahedron model has been developed in order to determine the effect of hydrogen on the visible–near-uv dielectric function of *a*-Si:H. The results of careful ir-absorption and film-density measurements have been utilized to obtain the concentrations and relative fractions of $Si\text{-}Si_4$, $Si\text{-}Si_3H$ (monohydride), and $Si\text{-}Si_2H_2$ (dihydride) tetrahedra present in the *a*-Si:H films studied. These results have indicated that random bonding of hydrogen, with no excess of $Si\text{-}H_2$, occurs for the $T_s = 250$ and 450 °C as-deposited films, but that nonrandom bonding with an excess of $Si\text{-}H_2$ occurs for the $T_s = 110$ °C film and for the annealed 250 ° film. This nonrandom bonding leads to the development of the two-phase microstructure discussed by other workers.

The use of these tetrahedron fractions along with the EMA yields predictions for ϵ_1 and ϵ_2 which are in good agreement with our own experimental results. Thus, this Si-centered tetrahedron model has been shown to provide a very useful framework for predicting ϵ_1 and ϵ_2 in the visible–near-uv region for these *a*-Si:H films. The necessary deposition conditions [$T_s = 250$ °C, $P(SiH_4) = 0.075$ Torr, power density of 0.15 W/cm^2] for random bonding of hydrogen and the suppression of excess $Si\text{-}H_2$ bonding have been confirmed.

ACKNOWLEDGMENTS

Research supported by the U.S. Department of Energy under Grant Nos. DE-FG02-84ER45168 and DE-FG02-87ER45317.

[1]M. H. Brodsky, M. Cardona, and J. J. Cuomo, Phys. Rev. B **16**, 3556 (1977).
[2]E. C. Freeman and W. Paul, Phys. Rev. B **20**, 716 (1979).
[3]D. Ewald, M. Milleville, and G. Weiser, Philos. Mag. B **4**, 291 (1979).
[4]K. Mui and F. W. Smith, Phys. Rev. B **35**, 8080 (1987); K. Mui, D. K. Basa, F. W. Smith, and R. Corderman, *ibid.* **35**, 8089 (1987); K. Mui, D. K. Basa, R. Corderman, and F. W. Smith, J. Non-Cryst. Solids **97/98**, 999 (1987).
[5]K. Mui and F. W. Smith, J. Appl. Phys. **63**, 475 (1988); J. Non-Cryst. Solids **97/98**, 975 (1987).
[6]D. A. G. Bruggemann, Ann. Phys. (Leipzig) **24**, 636 (1935).
[7]M. Cardona, Phys. Status Solidi B **118**, 463 (1983).
[8]H. Wagner and W. Beyer, Solid State Commun. **48**, 585 (1983).
[9]W. B. Pollard and G. Lucovsky, Phys. Rev. B **26**, 3172 (1982).
[10]H. Shanks, C. J. Fang, L. Ley, M. Cardona, F. J.Demond, and S. Kalbitzer, Phys. Status Solidi B **100**, 43 (1980).
[11]M. Ueda, A. Chayahara, T. Imura, Y. Osaka, M. Kumeda, and T. Shimizu, Jpn. J. Appl. Phys. **25**, 1148 (1986).
[12]K. K. Gleason, M. A. Petrich, and J. A. Reimer, Phys. Rev. B **36**, 3259 (1987).
[13]D. A. Anderson and W. Paul, J. Phys. Soc. Jpn., Suppl. A **49**, 1197 (1980); W. Paul, J. Phys. (Paris) Colloq. (Suppl. 10) **42**, C4-1165 (1981).
[14]B. G. Bagley, D. E. Aspnes, A. C. Adams, and C. J. Mogab, Appl. Phys. Lett. **38**, 56 (1981).
[15]B. G. Bagley, D. E. Aspnes, G. K. Celler, and A. C. Adams, in *Laser and Electron-Beam Interactions with Solids,* edited by B. R. Appleton and G. K. Celler (Elsevier Science, New York, 1982), p. 483.
[16]D. E. Aspnes, A. A. Studna, and E. Kinsbron, Phys. Rev. B **29**, 768 (1984). These results obtained in the range 1.5–6 eV have been extrapolated to 0 eV using the single oscillator expression [S. H. Wemple, J. Chem. Phys. **67**, 2151 (1977)].
[17]G. D. Cody, in *Semiconductors and Semimetals,* edited by J. I. Pankove (Academic, New York, 1984), Vol. 21, Pt. B, p. 11.
[18]J. C. Bruyere, A. Deneuville, A. Mini, J. Fontenille, and R. Danielou, J. Appl. Phys. **51**, 2199 (1980).
[19]H. R. Philipp, J. Phys. Chem. Solids **32**, 1935 (1971); J. Electrochem. Soc. **120**, 295 (1973).

[20]D. E. Aspnes and J. B. Theeten, J. Appl. Phys. **50**, 4928 (1979).
[21]A. Revesz, Thin Solid Films **50**, L29 (1978).
[22]J. C. Phillips, Phys. Rev. Lett. **20**, 550 (1968); Rev. Mod. Phys. **42**, 317 (1970).
[23]J. A. Van Vechten, Phys. Rev. **182**, 891 (1969); **187**, 1007 (1969).
[24]B. F. Levine, J. Chem. Phys. **59**, 1463 (1973).
[25]D. C. Allan and J. D. Joannopoulos, Phys. Rev. Lett. **44**, 43 (1980).
[26]C. J. Fang, L. Ley, H. R. Shanks, K. J. Gruntz, and M. Cardona, Phys. Rev. B **22**, 6140 (1980).
[27]K. Mui and F. W. Smith (unpublished).